energies

MDPI

Article

Dynamic TRM Estimation with Load–Wind Uncertainty Using Rolling Window Statistical Analysis for Improved ATC

Uchenna Emmanuel Edeh [1], Tek Tjing Lie [1,*] and Md Apel Mahmud [2]

[1] Department of Electrical and Electronic Engineering, Auckland University of Technology, Auckland 1010, New Zealand; uchenna.edeh@autuni.ac.nz
[2] College of Science and Engineering, Flinders University, Adelaide, SA 5001, Australia; apel.mahmud@flinders.edu.au
* Correspondence: tek.lie@aut.ac.nz

Abstract

The rapid integration of renewable energy sources (RES), particularly wind, together with fluctuating demand, has introduced significant uncertainty into power system operation, challenging traditional approaches for estimating Transmission Reliability Margin (TRM) and Available Transfer Capability (ATC). This paper proposes a fully adaptive TRM estimation framework that leverages rolling-window statistical analysis of net-load forecast errors to capture real-time uncertainty fluctuations. By continuously updating both the confidence factor and window length based on evolving forecast-error statistics, the method adapts to changing grid conditions. The framework is validated on the IEEE 30-bus system with 80 MW wind (42.3% penetration) and assessed for scalability on the IEEE 118-bus system (40.1% wind penetration). Comparative analysis against static TRM, fixed-confidence rolling-window, and Monte Carlo Simulation (MCS)-based methods shows that the proposed approach achieves 88.0% reliability coverage (vs. 81.8% for static TRM) while providing enhanced transfer capability for 31.5% of the operational day (7.5 h). Relative to MCS, it yields a 20.1% lower mean TRM and a 2.5% higher mean ATC, with an adaptation ratio of 18.8:1. Scalability assessment confirms preserved adaptation (12.4:1) with sub-linear computational scaling (1.82 ms to 3.61 ms for a 3.93× network size increase), enabling 1 min updates interval.

Keywords: available transfer capability (ATC); transmission reliability margin (TRM); Latin hypercube sampling (LHS); load forecasting; rolling window statistical analysis; uncertainty quantification; wind power forecasting

Academic Editor: Armando Pires

Received: 24 December 2025
Revised: 1 February 2026
Accepted: 3 February 2026
Published: 5 February 2026

1. Introduction

The global transition toward cleaner and more sustainable energy systems has accelerated the use of variable renewable energy sources (vRES), particularly wind and solar PV, into modern power grids. While this transformation supports decarbonization objectives and energy security goals, it fundamentally alters the uncertainty landscape of power system operations. Unlike conventional synchronous generators with deterministic output characteristics, renewable generation exhibits significant temporal variability driven by weather patterns, introducing forecast errors that can exceed 15 to 20% of installed capacity under extreme conditions [1,2]. Variability in renewable generation, fluctuating load demand, and dynamic transmission line capacities have become critical

factors that must be accounted for in real-time decision making to ensure secure and reliable grid operations. In response, advanced modeling and quantification frameworks—employing comprehensive uncertainty quantification and flexibility assessment—have been developed to assist grid operators and planners in managing these uncertainties more effectively. Simultaneously, demand-side dynamics have evolved beyond traditional predictable patterns due to the proliferation of distributed energy resources (DERs), electric vehicle (EV) charging infrastructure, and responsive or flexible loads. The confluence of supply-side and demand-side uncertainties necessitates the adoption of robust, data-driven analytical frameworks for real-time grid reliability assessment and operational decision making.

In this context, Available Transfer Capability (ATC) emerges as a critical operational metric that quantifies the additional power that can be reliably transferred over the transmission network without compromising system security. Defined by the North American Electric Reliability Corporation (NERC), ATC is derived from Total Transfer Capability (TTC) through the subtraction of existing transmission commitments (ETC), Capacity Benefit Margin (CBM), and the Transmission Reliability Margin (TRM), the latter serving as a buffer to accommodate system uncertainties [3–5]. Mathematically, ATC is given by Equation (1).

$$\mathrm{ATC} = \mathrm{TTC} - \mathrm{ETC} - \mathrm{CBM} - \mathrm{TRM} \quad (1)$$

where TTC is the total transfer capability, ETC is the existing transmission commitment, CBM is the capacity benefit margin and TRM is the transmission reliability margin.

Traditional TRM estimation approaches predominantly rely on fixed safety margins, typically calculated as a predetermined percentage of TTC or as static MW values based on historical operating experience [6,7]. While computationally simple, these deterministic methods introduce four key limitations in renewable-rich power systems. First, their static nature fails to reflect real-time fluctuations, often resulting in over- or underestimation of reserve needs. Second, these methods are frequently excessively conservative, which restricts market efficiency and transmission utilization. Third, temporal delays caused by manual update mechanisms cause the reserved capacity to not match actual risk levels. Fourth, and most importantly, deterministic approaches are insufficient for capturing risk in real time because they are unable to accurately quantify the probabilistic nature of load and renewable variability [8]. Despite advancements, probabilistic techniques like range-based TRM estimation still depend on static intervals and offline recalculations [6,9].

The development of dynamic TRM frameworks that can instantly adjust to shifting operating conditions has been motivated by these difficulties. However, there are still several research gaps in the current literature:

- Limited real-time adaptability in proposed probabilistic methods.
- Insufficient integration of multiple concurrent uncertainty sources.
- Lack of validated dynamic frameworks for operational implementation.
- Inadequate computational efficiency for online applications.

This study addresses the limitations of conventional TRM estimation methods by proposing a dynamic and fully adaptive TRM estimation framework based on rolling-window statistical analysis. The main contributions of this work are summarized as follows:

1. Fully Adaptive TRM Framework: Develop a dual adaptive TRM estimator where both rolling window length $W(t)$ and the confidence factor $K(t)$ are automatically updated using real-time volatility assessment.

2. Real-Time TRM Updating Capability: The proposed approach supports TRM estimation at operational timescales (minutes to hours), allowing reliability margins to dynamically adapt to evolving grid conditions rather than relying on static, offline margins.
3. Integrated Multi-Source Uncertainty Modeling and Validation: Load and wind uncertainties are jointly incorporated using LHS-based scenario generation, and the proposed framework is validated on a modified IEEE 30-bus system through comprehensive sensitivity analysis of key parameters.

The remainder of this paper is organized as follows: Section 2 reviews existing TRM estimation approaches and uncertainty modeling techniques. Section 3 details the proposed dynamic TRM framework, including rolling-window statistical modeling, LHS-based scenario generation, and adaptive window sizing. Section 4 describes the simulation setup and test system configuration. Section 5 presents the results and performance evaluation. Finally, Section 6 concludes the paper and outlines directions for future research.

2. Literature Review and Related Work

2.1. Transmission Reliability Margin: Theoretical Foundation and Operational Role

Transmission Reliability Margin (TRM), also known as security margin, serves as a fundamental reliability buffer in power system operations, accounting for uncertainties that conventional deterministic planning cannot capture. Probabilistic reliability assessment forms the theoretical foundation of TRM, providing a confidence margin that guarantees actual operating conditions, despite forecast deviations, maintain system security with a specified probability [10].

Conventionally, the assessment of available transfer capability has been a critical function in power system operations, relying predominantly on deterministic methods that assume fixed operating conditions. These approaches, while straightforward, often struggle to adequately capture the inherent variability and uncertainty introduced by the increasing penetration of renewable energy sources and fluctuating load demands [11]. As power systems transition towards higher renewable integration, the limitations of static, worst-case scenarios become apparent, frequently leading to overly conservative estimates or an underestimation of risks, thereby hindering economic efficiency and grid reliability. Maintaining reliability while managing increasing uncertainty has therefore become a key concern in the electric power sector's resource adequacy.

The practical implementation of the ATC formulation in Equation (1) requires careful coordination of all margin components. Specifically, underestimating TRM can lead to ATC overstatement and potential security violations, whereas overestimation constrains usable transfer capacity, thereby reducing market efficiency and economic welfare. Historically, utilities have used rule-of-thumb margins based on worst-case operational experience, which are usually 5–10% of TTC. Although they guarantee baseline security, such deterministic procedures are frequently unduly cautious and insensitive to changing system conditions.

According to a study [6], one approach to estimating TRM is to repeatedly compute TTC under different base-case conditions and use the range of outcomes to set a margin. While this range-based approach explicitly improves uncertainty awareness in margin estimation, it yields a single static value that requires offline recalculation. The fundamental limitation, therefore, remains the lack of adaptability to real-time operating conditions, such that conventional methods, whether simple deterministic rules or one-time probabilistic studies, cannot dynamically adjust to real-time evolving conditions and may struggle to adapt to high-volatility environments such as grids with large renewable

penetration. The need for more dynamic and responsive mechanisms is evident, especially considering the continuous evaluation required for probabilistic dynamic security assessment in large power systems with variable loads and generation.

2.2. Modeling and Quantification of Uncertainty in Power Systems

Reliable power-system operation requires continuous and accurate quantification of uncertainty arising from both supply-side and demand-side variations. These uncertainties directly affect nodal power injections, transmission line flows, reserve allocation, and operational security margins, forming the foundation for probabilistic TRM assessment [12,13]. In modern power systems with high penetration of renewable energy sources (RES), uncertainty is inherently multi-dimensional, nonlinear, correlated, and time-varying, rendering conventional static margin approaches increasingly inadequate.

Power-system uncertainty is commonly classified into aleatory and epistemic components [14]. Aleatory uncertainty originates from the inherent randomness of physical processes, such as wind-speed fluctuations, short-term load variability, and solar irradiance intermittency. These uncertainties are irreducible and must be characterized using stochastic probability distributions. Epistemic uncertainty, in contrast, arises from incomplete system knowledge, parameter estimation errors, and modeling simplifications. Although reducible in principle, epistemic uncertainty remains significant in operational contexts due to data latency, forecast imperfections, and evolving grid conditions [11,13].

Among all uncertainty sources, forecast-related uncertainty has emerged as one of the most influential factors in renewable-rich power systems. Deviations in day-ahead and short-term forecasts of wind and solar generation introduce non-Gaussian fluctuations that propagate directly into ATC and TRM calculations [15]. Empirical studies demonstrate that forecast errors exhibit temporal autocorrelation, regime-dependent behavior, and asymmetric distributions, challenging the validity of fixed confidence-factor assumptions traditionally adopted in TRM estimation. Consequently, recent research emphasizes a transition from point forecasts toward probabilistic forecasting frameworks that explicitly quantify uncertainty through prediction intervals or full probability density functions. Joint probabilistic forecasting of demand and renewable generation has further been shown to improve system-level uncertainty representation in operational studies.

Additional uncertainty arises from topology changes and contingencies, such as unexpected line outages, generator trips, or switching activities. These events modify the network configuration instantaneously, affecting TTC, line loading, and sensitivity factors, and thereby influencing the TRM requirement. Increasing electrification, particularly from large-scale EV charging demand, further adds stochastic stress on distribution and transmission networks.

Correlated uncertainties are increasingly recognized as a critical feature of modern power systems. Wind farms located within the same meteorological region exhibit strong spatial and temporal correlation, while load demand responds coherently to temperature, socio-economic activity, and consumer behavior. Renewable–load interactions further introduce joint variability that cannot be adequately captured under independent distribution assumptions. Neglecting these dependencies can lead to systematic overestimation or underestimation of TRM. Recent studies demonstrate that ignoring wind-speed spatiotemporal correlation results in biased ATC estimation in wind-integrated transmission corridors. The principal challenge is generating uncertainty scenarios that preserve marginal distributions and cross-correlations among wind, solar, and load while remaining computationally efficient for operation.

Conventional deterministic frameworks approximate uncertainty through fixed worst-case margins or offline probabilistic studies. However, static approaches fail to capture rapid volatility shifts, evolving correlations, and non-stationary uncertainties in high-

RES systems. Recent evidence shows that deterministic TRM rules can misrepresent security requirements under fast-changing operating conditions, especially during high renewable variability [10]. These limitations motivate probabilistic, data-driven, and time-adaptive uncertainty modeling approaches, forming the basis of the dynamic rolling-window TRM methodology developed in this paper.

2.3. Probabilistic and Statistical Techniques for TRM Estimation

The limitations of deterministic TRM approaches have motivated a wide range of probabilistic and statistical methods. Among these, Monte Carlo Simulation (MCS) is widely used, generating random scenarios that capture fluctuations in load, renewable generation, and contingencies [10,16]. By evaluating the distribution of resulting ATC values, TRM can be selected to satisfy a target reliability level, such as ensuring that 95% of scenarios meet security constraints. Although rigorous, MCS requires thousands of power-flow computations to achieve stable results, limiting its applicability in real-time or high-frequency settings. In addition, rare but operationally significant events may be insufficiently represented, potentially underestimating system risk.

To reduce computational burden, LHS stratifies the input probability space, generating representative scenarios with far fewer samples [17,18]. By uniformly covering uncertainty domains, LHS significantly reduces variance relative to random sampling, improving the feasibility of near-real-time probabilistic TRM estimation.

Beyond MCS and LHS, several advanced probabilistic frameworks have been explored in the recent literature. Parametric bootstrap methods resample data to quantify parameter uncertainty but often rely on fixed historical distributions [19]. Bayesian Networks model probabilistic dependencies and support online updates, but their computational demands limit real-time use [20]. Stochastic Process Models, such as Markov chains and stochastic Petri nets, capture temporal correlations but face challenges in parameter validation and computational efficiency. Interval and robust methods yield conservative margins without full probability distributions; however, they lack explicit confidence levels and may result in overly cautious TRM estimates. To contextualize these limitations, Table 1 presents a comparative summary of existing major probabilistic methods for TRM assessment.

Table 1. Comparison of major probabilistic methods for TRM assessment.

Method	Description	Strengths	Limitations
Monte Carlo Simulation (MCS)	Random sampling to obtain ATC/TRM distributions	Rigorous; widely validated	Computationally heavy; impractical for real-time
Latin Hypercube Sampling (LHS)	Stratified sampling of uncertainty distributions	High efficiency; reduced variance	Still offline; assumes static distributions
Bootstrap-Based Methods	Resampling historical data or assumed distributions	Statistically robust	Limited adaptiveness under changing conditions
Bayesian Networks	Probabilistic dependency modeling	Captures correlations; supports updating	High computation and data requirements
Stochastic Process Models (Markov chains, Petri nets)	Temporal correlation modeling via state transitions	Captures sequential dependencies	Parameter validation challenges; execution time
Interval/Robust Methods	Bounded uncertainty sets without full distributions	Conservative guarantees; computationally tractable	No explicit confidence levels; potentially over-conservative

Although these probabilistic techniques represent major progress compared to deterministic TRM estimation, they share common limitations: (i) offline computation, (ii) fixed or assumed uncertainty distributions, and (iii) limited adaptability to evolving system conditions.

These limitations necessitate the development of dynamic, data-driven frameworks capable of continuously adjusting TRM to reflect changing operating environments.

2.4. Renewable Integration and Time-Varying Uncertainty

Large-scale integration of renewable energy, particularly wind, has introduced unprecedented variability and forecast uncertainty into modern power systems [21]. Wind generation often fluctuates rapidly, with variations exceeding 50% of installed capacity over short time intervals during frontal weather events. Forecast accuracy deteriorates during high-volatility periods, with day-ahead RMSE values commonly ranging between 10 and 15% and increasing to 15–25% for hour-ahead forecasts. Spatial correlations among geographically proximate wind farms further increase system-level uncertainty and diminish the smoothing benefits of geographical diversification. Seasonal and diurnal meteorological patterns also contribute to time-varying forecast error characteristics [22].

Simultaneously, modern load behavior is becoming increasingly uncertain due to the proliferation of distributed energy resources, electric vehicle charging patterns, and demand-response participation. Power systems now experience bidirectional uncertainty, where both supply and demand fluctuate dynamically across short timescales—conditions under which static TRM approaches become ineffective.

The correlated variability of renewable generation and dynamic load demand exposes several limitations of traditional TRM methodologies. Fixed confidence margins often become insufficient during periods of severe volatility, yet overly conservative under stable conditions, leading to either increased risk or inefficient use of transmission capacity. Moreover, infrequent TRM updates create temporal mismatches between the assumed and actual uncertainty environments.

Recent findings increasingly demonstrate that TRM must vary with time and expand or contract based on evolving operating conditions [9,23]. Static approaches fail to capture this adaptive behavior, which is essential for maintaining reliability while maximizing available transfer capability.

2.5. Dynamic and Adaptive TRM: Emerging Paradigms

In response to these challenges, dynamic TRM methodologies have gained significant attention, particularly those employing rolling-window statistical analysis. Under this paradigm, TRM is recalculated periodically using a sliding window of recent system data—typically spanning 20 to 60 min—allowing the margin to track short-term fluctuations in uncertainty [9,23]. Rolling-window methodologies offer several operational advantages:

1. Real-Time Responsiveness: TRM values adapt immediately to rapid changes in renewable volatility, load fluctuations, and forecast error characteristics.
2. Data-Driven Objectivity: Margins reflect observed uncertainty rather than subjective worst-case assumptions, reducing unnecessary over-provisioning.
3. Computational Efficiency: Calculations rely on simple statistics (e.g., mean and variance), making them suitable for real-time implementation.
4. Automatic Adaptation to Regime Shifts: As underlying conditions evolve—such as seasonal transitions or sudden weather changes—rolling-window methods require no manual recalibration.

Advanced adaptive-windowing approaches, such as ADWIN [24], further enhance responsiveness by dynamically resizing the effective window length when detecting distributional drift. Evidence from related domains, including financial volatility modeling and data-center load forecasting, shows that adaptive windowing outperforms fixed-window methods under non-stationary conditions.

Despite these advances, many dynamic TRM studies lack validation on realistic test systems, offer limited sensitivity analyses, and rarely demonstrate real-time computational feasibility. Moreover, the joint treatment of multiple uncertainty sources, including renewable generation, load, and network conditions, remains underexplored.

These research gaps motivate the present work, which develops and validates a multi-source, fully adaptive rolling-window TRM estimation framework designed for operational deployment in renewable-rich power systems.

3. Proposed Methodology

This section presents a multi-source, adaptive rolling-window framework for real-time estimation of TRM under uncertainty. The proposed methodology integrates probabilistic uncertainty modeling, scenario generation, and a volatility-responsive rolling window to drive time-varying TRM values suitable for renewable-rich power systems. By dynamically adapting to evolving operating conditions, the framework enables responsive and data-driven reliability margin estimation. The overall workflow of the proposed methodology is summarized in Figure 1.

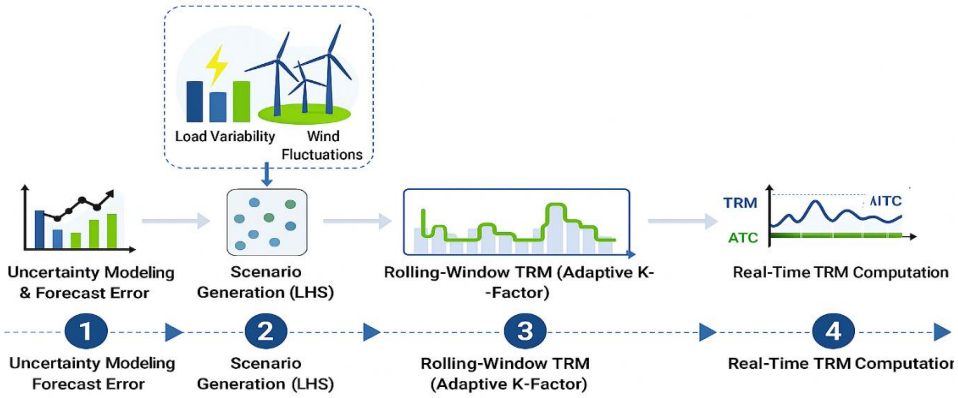

Figure 1. Conceptual workflow of the multi-source adaptive rolling-window TRM estimation framework.

Table 2 presents the modified IEEE 30-Bus test system configuration.

Table 2. Modified IEEE 30-bus test system configuration.

Parameter	Value	Description
Test System	30	Standard IEEE 30-bus topology
Generators	6	Conventional units at buses 1, 2, 5, 8, 11, 13 (Exporting Area)
Wind farms	2	Integrated on buses 14 and 16 (Importing Area)
Wind capacity	80 MW	40 MW each on buses 14 and 16
Total load	283.4 MW	Base case loading
Branches	41	Transmission lines and transformers
Solver	MATPOWER	AC power flow using Newton-Raphson method
Transfer corridor	Area 1 → 2	Tie-lines: 12–15, 12–16, 14–15, 15–18, 15–23

The modified IEEE 30-bus test system used for validation is illustrated in Figure 2, highlighting the exporting and importing areas.

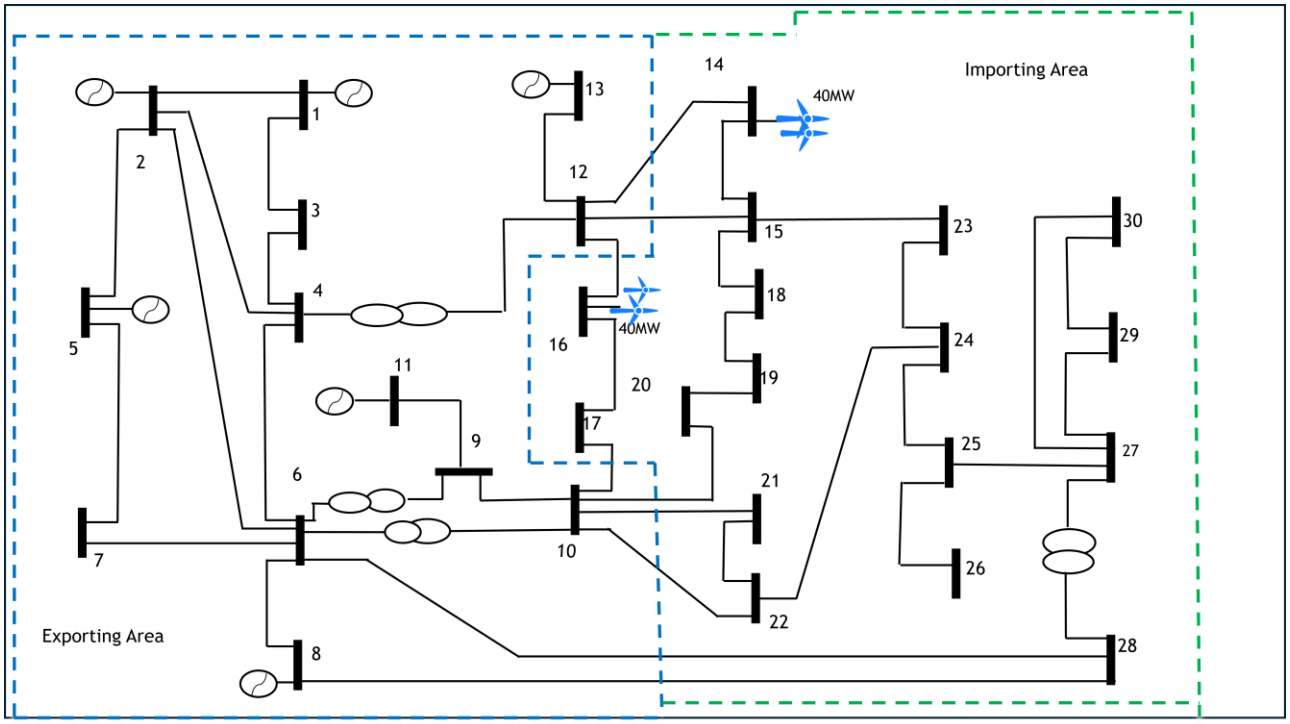

Figure 2. Single-line diagram of the modified IEEE 30-bus test system showing exporting (Area 1, shaded in blue) and importing areas (Area 2, shaded in green).

As shown in Figure 3, the system exhibits pronounced diurnal and stochastic behavior over the 24 h study horizon.

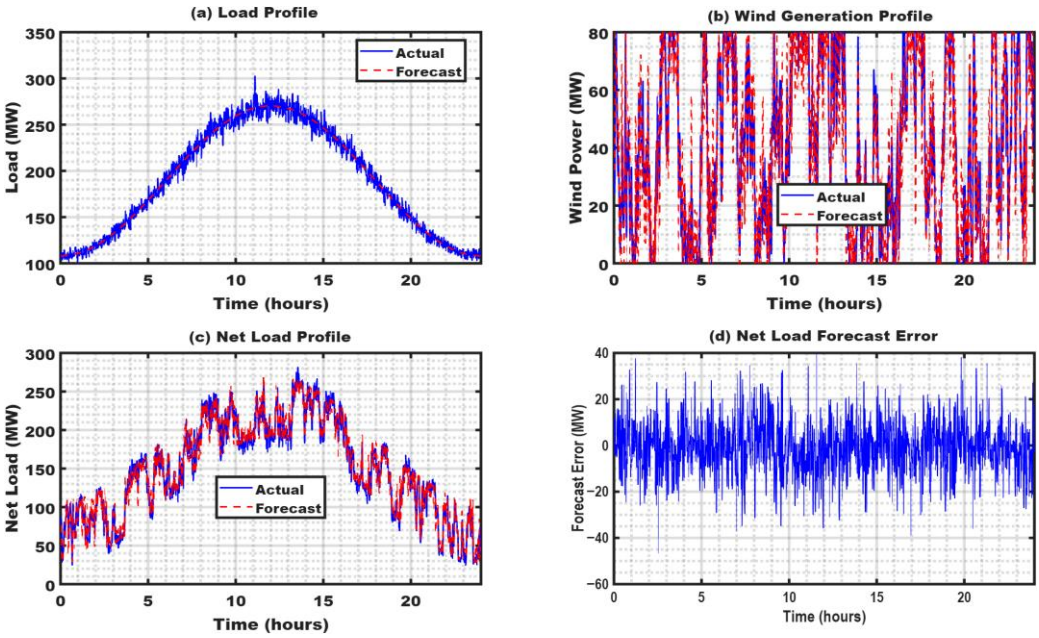

Figure 3. System profiles over a 24-hour study horizon: (**a**) load profile with actual and forecast values showing diurnal variation with midday peak demand; (**b**) wind power output; (**c**) net load (load minus wind generation); (**d**) net load forecast error.

The system is divided into two areas (see Figure 2). The Exporting Area (buses 1–15) serves as the generation/export region containing all conventional generators, while the Importing Area (buses 16–30) represents the load/import area where wind farms are integrated. This configuration reflects realistic operating scenarios in which remote renewable

generation is geographically separated from load centers, analogous to distributed wind resources offsetting local demand. The base-case TTC is determined based on the aggregate thermal capacity of the tie-line corridor, with a 75% utilization factor applied to provide a conservative operating margin.

3.1. Uncertainty Modeling and Forecast Error Generation

Two primary sources of short-term uncertainty are considered: load demand variability and wind generation fluctuations. Their probabilistic characteristics follow widely established models.

3.1.1. Load Demand Uncertainty

Short-term load variations are commonly assumed to follow near-Gaussian distributions, supporting normal distribution modeling as expressed in (2) [25].

$$f_L(P_L) = \frac{1}{\sigma_L\sqrt{2\pi}}\, exp\left(-\frac{(P_L-\mu_L)^2}{2{\sigma_L}^2}\right) \tag{2}$$

where P_L is the actual load, μ_L is the expected (forecast) load, σ_L is the forecast error standard deviation, and $f_L(P_L)$ is the probability density function (pdf) of P_L. Empirical studies report σ_L values of 2–5% for hour-ahead forecasts and 5–8% for day-ahead horizons. In this study, $\sigma_L = 3\%$ of the mean load is adopted for the base case.

3.1.2. Wind Speed and Power Uncertainty

Wind speed v is modeled using a two-parameter Weibull probability distribution, which has been shown to provide a robust fit for many wind-regime datasets [26]. The probability density function is given by (3).

$$f_v(v) = \frac{k}{c}\left(\frac{v}{c}\right)^{k-1} \exp\left[-\left(\frac{v}{c}\right)^{k}\right] \tag{3}$$

where k and c are the shape and scale parameters, respectively, and v is the wind speed. For this study, k = 2.0 and c = 8 m/s are adopted based on typical onshore wind characteristics. The Weibull distribution flexibly represents diverse wind regimes via its parameters: the shape parameter k typically ranges from 1.5 to 3.0, and $k = 2$ reduces the Weibull distribution to the Rayleigh distribution (a special case), while the scale parameter c is proportional to the mean wind speed.

Wind-to-power conversion is modeled using the standard piecewise turbine power curve as shown in (4).

$$P_{wind}(v) = \begin{cases} 0, & v < v_{ci,} \\ P_r\dfrac{v - v_{ci}}{v_r - v_{ci}}, & v_{ci} \le v < v_r, \\ P_r, & v_r \le v < v_{co,} \\ 0, & v \ge v_{co}, \end{cases} \tag{4}$$

where v_{ci}, v_r, and v_{co} denote the cut-in, rated, and cut-out wind speeds, respectively, and P_r represents the turbine rated power. In this study, $v_{ci} = 3$ m/s, $v_r = 12$ m/s, and $v_{co} = 25$ m/s.

3.1.3. Net Load Formulation and Forecast Error Characterization

To capture the combined effect of load and wind uncertainty, the net load formulation is adopted. The net load at time t is defined by (5).

$$P_{netLoad,t} = P_{Load,t} - P_{wind,t} \quad (5)$$

where $P_{netLoad,t}$ is the residual system demand after accounting for wind generation, $P_{Load,t}$ is the total system load demand at time t, and $P_{wind,t}$ is the total wind power generation at time t.

Forecast uncertainty in this study is quantified using the empirical deviation between baseline forecasts and actual observed system quantities. At each time step t, the forecast error is evaluated using (6).

$$e_t = P_{actual,t} - P_{forecast,t} \quad (6)$$

where $P_{Forecast,t}$ is the reference forecast (load, wind, or net load) and $P_{Actual,t}$ is the realized value. The error sequence $\{e_t\}$ is treated as a zero-mean, time-varying stochastic process, whose variance reflects evolving operational and meteorological conditions.

3.1.4. Persistent Day-Ahead Forecasting

The baseline forecast used in (6), is generated using a Persistence Day-Ahead Forecasting Model, which is widely employed as a benchmark in power system forecasting studies due to its simplicity and effectiveness. In this study, day-ahead forecasts are generated for wind power generation and system load demand, which are the primary sources of short-term uncertainty affecting TRM estimation. This benchmark approach is widely used to characterize forecast errors due to its simplicity and transparency. The forecast for the current time step is defined by (7).

$$P_{forecast,t} = P_{actual,t-24\,\mathrm{h}} \quad (7)$$

Under the persistence model, forecast errors exhibit the following characteristics:

- Magnitude: RMSE values of 10–20% for wind power and 3–8% for load demand.
- Temporal Correlation: Autocorrelation structures reflecting weather persistence and demand patterns.
- Non-Stationarity: Error variance varies with time of day, season, and meteorological conditions.

3.2. Stochastic Scenario Generation Using Latin Hypercube Sampling

The LHS technique is employed to efficiently generate representative uncertainty scenarios for joint load–wind variability. LHS stratifies each marginal distribution into equally probable intervals and draws one sample from each stratum ensuring comprehensive coverage [27].

For M load intervals and N wind intervals, the total number of scenarios is $K = M \times N$. Each scenario (i, j) is assigned a probability weight as shown in (8).

$$\pi_{ij} = \pi_i^{(load)} \times \pi_j^{(wind)} \quad (8)$$

where $\pi_i^{(load)} = 1/M$ and $\pi_j^{(wind)} = 1/N$ under equal-probability stratification.

The Implementation procedure is summarized in (9) and (10) as follows:

1. Generate M quantile points for load distribution as shown in (9).

$$q_i^L = F_L^{-1}\left(\frac{i}{M+1}\right), i = 1, \ldots, M. \quad (9)$$

2. Generate N quantile points for wind distribution as shown in (10).

$$q_j{}^W = F_V{}^{-1}\left(\frac{j}{N+1}\right), j = 1, \ldots, N. \quad (10)$$

3. Randomly permute wind quantiles to eliminate artificial correlation while maintaining stratified coverage.
4. Form $K = M \times N$ scenario pairs $\left(q_i{}^L, q_j{}^W\right)$ with associated probabilities π_{ij}.

This approach ensures representative coverage of the joint probability space with substantially fewer scenarios than conventional random or Monte Carlo sampling, thereby improving computational efficiency for real-time TRM assessment.

3.3. Rolling-Window Statistical Framework

The rolling-window approach characterizes real-time volatility in forecast error using a sliding window of length W that maintains the most recent error samples $\{e_t - W + 1, \ldots, e_t\}$. This is illustrated in Figure 4.

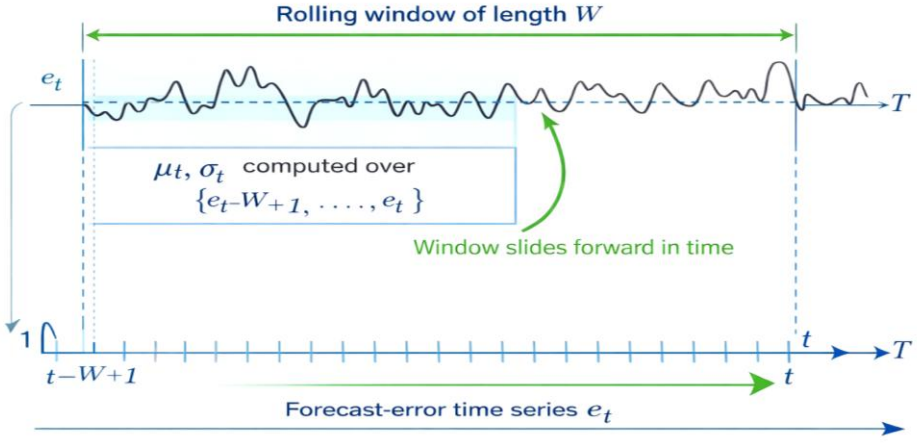

Figure 4. Illustration of the rolling-window statistical framework applied to the forecast error time series. A fixed- length window W slides forward in time, and the rolling mean μ_t and standard deviation σ_t are computed over the most recent samples $\{e_t - W + 1, \ldots, e_t\}$.

3.3.1. Rolling-Mean and Standard Deviation

Within each window, the rolling mean μ_t and standard deviation σ_t are computed using (11) and (12), where e_t represents forecast error at time t.

$$\mu_t = \frac{1}{W}\sum_{i=t-W+1}^{t} e_t \quad (11)$$

$$\sigma_t = \sqrt{\frac{1}{W-1}\sum_{t-W+1}^{t}(e_t - \mu_t)^2} \quad (12)$$

3.3.2. Adaptive Confidence Factor

To address the limitations of fixed confidence factors in non-stationary environments, an adaptive confidence factor, $K(t)$, is defined by (13).

$$K(t) = K_{base} \times \left[1 + \beta \left(\frac{\sigma_t - \sigma_{ref}}{\sigma_{ref}}\right)\right] \quad (13)$$

where K_{base} is the baseline confidence factor (95% confidence under Gaussian assumptions), σ_{ref} is the reference standard deviation from a historical calibration period, σ_t is the current rolling-window standard deviation, and β is the adaptive scaling coefficient.

3.3.3. Scaling Coefficient β

The scaling coefficient β captures the relative contribution of wind-power variability to overall system uncertainty and is derived empirically as shown in (14).

$$\beta = \frac{\sigma_{wind}}{\sigma_{netload}} = \frac{\sqrt{Var(P_{wind})}}{\sqrt{Var(P_{netload})}} \quad (14)$$

where $Var(P_{wind})$ and $Var(P_{netload})$ denote the Variances of wind power generation and net load over the study period, respectively.

Figure 5 illustrates the temporal evolution of the adaptive confidence factor and rolling forecast-error volatility under time-varying operating conditions.

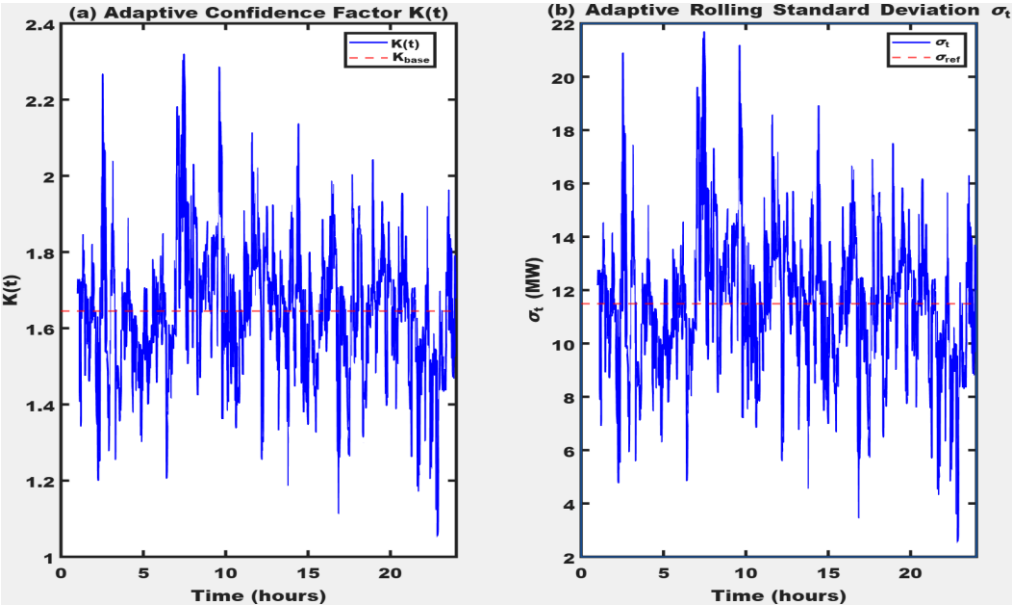

Figure 5. Time-varying adaptive confidence factor $K(t)$ and the corresponding rolling standard deviation σ_t over 24 h simulation horizon. Subplot (**a**) shows the evolution of the adaptive. confidence factor, while subplot (**b**) presents the associated rolling standard deviation of forecast error, highlighting periods of elevated system uncertainty.

3.4. Window Size Sensitivity Analysis

(1) Fixed Window Size Analysis

To determine the baseline window size, window lengths of $W \in \{15, 30, 45, 60\}$ minutes were evaluated. These values reflect common operational timescales used in modern power systems:

- 15 min—typical for automatic generation control (AGC); highly responsive.
- 30 min—consistent with real-time dispatch and short-term balancing actions.

- 60 min—representative of hourly scheduling; produces smoother but slower estimates.

(2) Rolling RMSE Evaluation

For each fixed window W, the rolling Root Mean Square Error (RMSE) of forecast performance is computed using (15).

$$\mathrm{RMSE_t}(W) = \sqrt{\frac{1}{W}\sum_{i=t-W}^{t}\left(P_{forecast,i} - P_{actual,1}\right)^2} \tag{15}$$

where $P_{forecast,i}$ and $P_{actual,i}$ represent the forecasted and actual quantities (e.g., load or wind power) at time i.

This evaluates how each window manages the trade-off between noise filtering volatility tracking.

Trade-off Insight:

- Shorter windows (10–15 min) respond quickly to changes but are more sensitive to noise.
- Longer windows (60 min) produce stable estimates but may lag rapid fluctuations.
- Intermediate windows (30–45 min) typically strike a practical balance between stability and responsiveness.

The final baseline window W_{base} will be selected based on the observed RMSE behavior and its ability to capture volatility without introducing unnecessary noise.

3.5. Adaptive Window Sizing Mechanism

To accommodate rapid fluctuations in forecast error volatility, the window length $W(t)$ is adapted dynamically based on the volatility change rate as shown in (16).

$$R(t) = \frac{\sigma_t - \sigma_{t-\Delta t}}{\sigma_{t-\Delta t}} \tag{16}$$

The adaptive window is then computed using (17).

$$W(t) = W_{base} - \alpha|R(t)| \tag{17}$$

The adjustment coefficient α determines the sensitivity of the window to volatility variations and is obtained empirically as shown in (18).

$$\alpha = \frac{W_{base} - W_{min}}{|R|_{max}} \tag{18}$$

where W_{base} is the baseline window, W_{min} is the minimum allowable window, and $|R|_{max}$ is the maximum observed volatility change rate computed as the 95th percentile of $|R(t)|$ from the calibration dataset to avoid undue influence from extreme outliers. This formulation ensures that $W(t)$ contracts to W_{min} under maximum volatility and remains at W_{base} during stable conditions, improving responsiveness and statistical reliability for robust estimation of TRM [28].

The window is bounded by (19).

$$W_{min} \le W(t) \le W_{max} \tag{19}$$

where W_{min} = 15 min ensures statistical validity (minimum 15 samples) and W_{max} = 60 min aligns with hourly operational planning cycles.

Figure 6 illustrates the adaptive window dynamics over the 24 h simulation horizon.

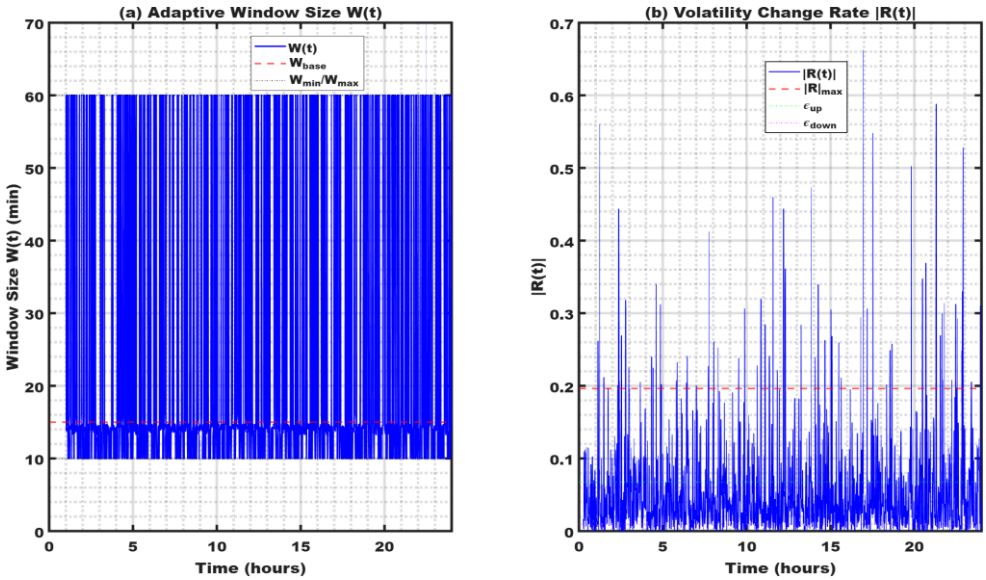

Figure 6. Adaptive window length $W(t)$ and corresponding volatility change rate $|R(t)|$ over the 24 h simulation horizon. (**a**) Time-varying adaptive window size $W(t)$. (**b**) Volatility change rate $|R(t)|$, illustrating how the window contracts and expands in response to real-time variability governed by Equations (15)–(18).

3.6. Dynamic TRM Formulation

The dynamic TRM at time (t) is computed using the adaptive confidence factor $K(t)$ introduced in (13) and the optimized rolling window standard deviation $\sigma_{e,t}$ as defined in (12). The resulting dynamic TRM is as shown in (20).

$$TRM_t = K(t) \times \sigma_{e,t} \tag{20}$$

where $\sigma_{e,t}$ represents the standard deviation of the forecast error at time t.

This formulation enables TRM to adapt in real time to fluctuations in system uncertainty, capturing variations arising from both load and renewable generation. Unlike conventional static TRM approaches that assume constant uncertainty levels, the proposed dynamic TRM adjusts the reliability margin in response to evolving system operation conditions, thereby improving operational reliability, responsiveness and statistical robustness.

3.7. ATC Formulation

The Available Transfer Capability (ATC) at time t is calculated in accordance with the standard NERC definition [7] as given by (21).

$$ATC_t = TTC - ETC - TRM_t \tag{21}$$

where TTC is the Total Transfer Capability, ETC represents the Existing Transmission Commitments, and TRM_t is the dynamic Transmission Reliability Margin obtained from (20).

This formulation ensures that ATC reflects real-time system conditions by explicitly accounting for committed transfers and the dynamically adjusted reliability margins, thereby providing a robust and risk-aware basis for operational decision making in power systems with high renewable energy penetration.

4. Simulation Results and Discussion

This section presents a comprehensive quantitative evaluation of the proposed dynamic and fully adaptive TRM estimation framework. The analysis covers (i) simulation

configuration and base-case operating point, (ii) validation of the adopted Latin Hypercube Sampling (LHS) resolution, (iii) window-size sensitivity and derived adaptive parameters, and (iv) benchmarking against representative static, rolling-window, and probabilistic TRM methods. Reliability preservation is assessed using coverage probability and Loss of Load Probability (LOLP), and computational timing is reported to support real-time feasibility.

4.1. Simulation Parameters and Test System Configuration

All simulations were conducted on the IEEE 30-bus test system with wind generation integrated at Buses 14 and 16. Steady-state AC power flow was solved in MATPOWER using the Newton–Raphson algorithm. A single transfer corridor was defined between an export area (Buses 1–13) and an import area (Buses 14–30). The study horizon was 24 h with a temporal resolution of 1 min (1440 steps).

Uncertainty was introduced through probabilistic load and wind forecast errors generated using LHS. The baseline confidence factor was set to $K_{base} = 1.645$ (95% confidence), and rolling-window bounds were defined as 10–60 min. A baseline window of 15 min was selected via sensitivity analysis (Section 4.4). Key simulation parameters are summarized in Table 3.

Table 3. Summary of complete simulation parameters.

Parameter	Value	Description
Time horizon	24 h	One full operational day
Time step (Δt)	1 min	High-resolution temporal granularity
LHS scenarios	100	M = 10 load × N = 10 wind intervals
Baseline window (W_{base})	15	Selected from sensitivity analysis
Baseline confidence (K_{base})	1.645	95% confidence level
Window bounds	10–60 min	W_{min} to W_{max}

4.2. Base-Case System Characteristics

Base-case power-flow results are summarized in Table 4. The total system load is 189.2 MW and wind generation is 80 MW, corresponding to a wind penetration of 42.3%. The base inter-area transfer (export to import) is −56.50 MW, and nine tie-lines were identified across the corridor.

The TTC was computed as 216.0 MW based on binding thermal constraints on the inter-area corridor. This confirms that the corridor is thermally constrained and that the adopted TTC reflects a realistic operational upper bound for ATC calculations under the simulated operating conditions. Base-case system characteristics are summarized in Table 4.

Table 4. Base case power flow results.

Parameter	Value
Total system load	189.2 MW
Wind generation	80 MW
Wind penetration	42.3%
Base transfer (Export → Import)	−56.50 MW
Total Transfer Capability (TTC)	216 MW
Number of tie-lines identified	9

4.3. LHS Scenario Convergence Analysis

To justify the adopted LHS resolution $(M = 10, N = 10, K = 100)$, a convergence study was conducted by increasing the scenario count from $K = 25$ to $K = 625$ and monitoring the stability of the estimated standard deviation of net-load samples together with computation time. Results are reported in Table 5 and the convergence behavior of the LHS scenarios, and the associated computational cost are illustrated in Figure 7.

Increasing from $K = 25$ to $K = 100$ reduces the estimated standard deviation from 15.89 MW to 12.41 MW (21.86% change). Beyond $K = 225$, relative changes fall below 5%, while computation time increases. This validates the choice of $K = 100$ as a practical compromise between statistical stability and computational efficiency.

Table 5. LHS convergence analysis.

M	*N*	*K* (Total)	σ (MW)	Relative Change (%)	Time (ms)
5	5	25	15.89	0	12.13
10	10	100	12.41	21.86	6.33
15	15	225	12.93	4.15	5.48
20	20	400	13.20	2.10	6.38
25	25	625	13.29	0.69	12.50

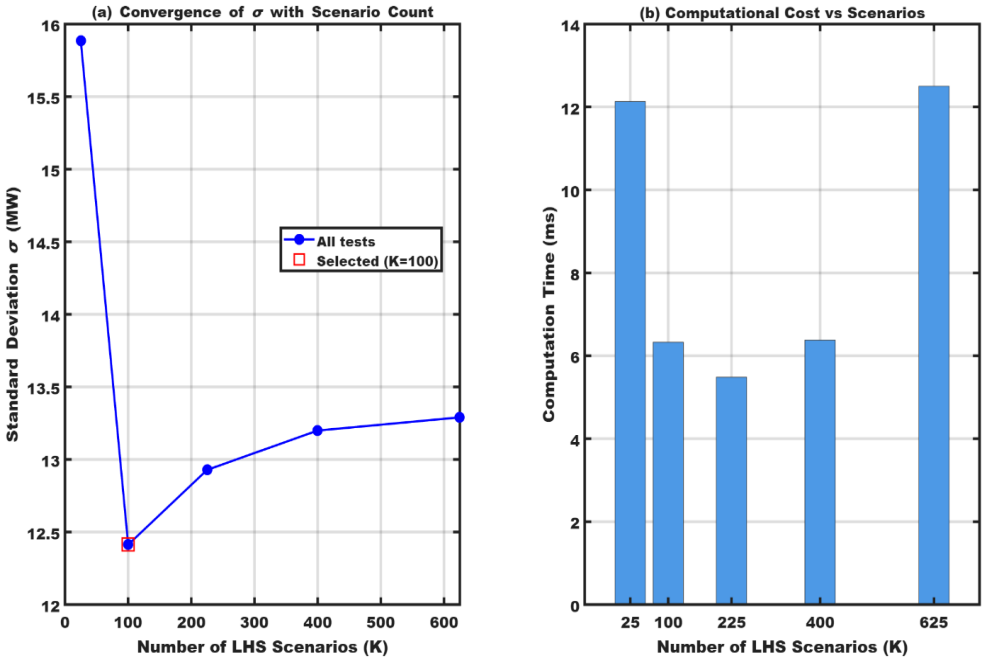

Figure 7. LHS convergence analysis: (**a**) estimated standard deviation σ versus scenario count K; (**b**) computation time versus scenario count K. The selected configuration $K = 100$ is highlighted.

4.4. Window Size Sensitivity and Baseline Window Selection

Because the proposed framework relies on rolling-window statistics, the window length must balance noise amplification (small windows) against excessive smoothing (large windows). A sensitivity analysis was conducted for fixed windows within the operationally feasible range of 10–60 min. Results are summarized in Table 6. Figure 8 provides a visual comparison of the window-size impact on (a) average RMSE with variability (standard deviation error bars) and (b) the rolling RMSE trajectories over the 24 h horizon.

The 10 min window yields the lowest mean RMSE (11.60 MW), indicating strong responsiveness. However, it also exhibits the highest variability (Std RMSE = 3.10 MW), suggesting increased sensitivity to short-term noise. The 15 min window provides a near-

minimum mean RMSE (11.76 MW) with improved stability (Std RMSE = 2.61 MW), offering a more robust accuracy–stability trade-off for operational use. Larger windows (30–60 min) further reduce RMSE variability but slightly increase mean RMSE, reflecting smoother yet less responsive estimates.

Based on these results, the baseline window was set to $W_{base} = 15$ min.

Table 6. Window size sensitivity results.

Window Size (min)	Mean RMSE (MW)	Std RMSE (MW)
10	11.60	3.10
15	11.76	2.61
30	11.91	1.88
45	11.94	1.63
60	11.95	1.46

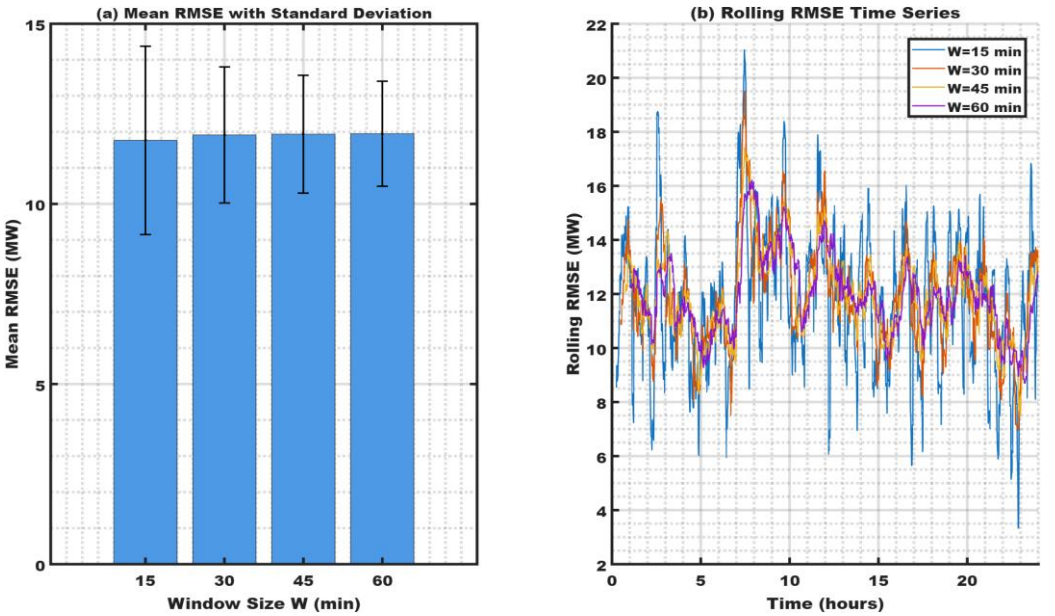

Figure 8. Window size sensitivity analysis: (**a**) Average RMSE with standard deviation error bars for window sizes, and (**b**) rolling RMSE time series over the 24 h horizon.

4.5. Calibration of Adaptive Parameters from Rolling Statistics

Adaptive parameters governing confidence factor adjustment and volatility-driven window modulation/shifting were computed from rolling statistics of net-load forecast errors. The results obtained are reported in Table 7. The wind-variability ratio $\beta = 0.4618$ indicates that wind-power fluctuations account for approximately 46% of total net-load variability. The reference standard deviation $\sigma_{ref} = 11.49$ MW represents the full-day average of the rolling forecast-error standard deviation. The window-adjustment factor $\alpha = 25.47$ governs the contraction and expansion of $W(t)$, while the maximum volatility rate $|R|_{max} = 0.1963$ (95th percentile) defines the upper bound for volatility-driven window modulation.

Table 7. Derived adaptive parameters.

Parameter	Symbol	Value	Description
Wind variability ratio	B	0.4618	Ratio of wind to net-load variability
Reference std dev.	σ_{ref}	11.49 MW	Daily avg. of rolling σ_t

Window adjustment factor	A	25.47	Controls window contraction rate
Max volatility rate	$\lvert R(max) \rvert$	0.1963	95th percentile of $\lvert R(t) \rvert$
Historical forecast error std	$\sigma_{hist.}$	12.02 MW	Overall forecast error std dev.

4.6. Benchmark Set and Baseline Definition (4 Approaches)

Four TRM formulations were assessed to position the proposed method relative to established industry practice and to highlight the role of adaptive confidence adjustment:

1. Static TRM (Industry Practice): $\text{TRM} = 0.075 \times \text{TTC}$.
2. Fixed-K Rolling (Baseline): adaptive window $W(t)$ with fixed $K = 1.645$.
3. MCS-Based TRM: TRM obtained from the 95th percentile of absolute forecast error using $N = 1000$ samples.
4. Proposed Adaptive TRM: both $W(t)$ and $K(t)$ are adaptive.

The Fixed-K Rolling method is used as the key baseline because it retains adaptive windowing while removing adaptive confidence adjustment, thereby enabling direct attribution of performance differences to the proposed $K(t)$ mechanism.

4.7. Comparative TRM and ATC Performance

Performance statistics across all four methods are summarized in Table 8. The static TRM yields a constant margin of 16.20 MW and a mean ATC of 199.80 MW but exhibits inadequate reliability (81.8% coverage; LOLP of 18.2%). Introducing adaptivity through the fixed-K rolling method improves reliability to 88.4% coverage with a mean TRM of 18.77 MW and a mean ATC of 197.23 MW, indicating the benefit of adaptive windowing alone.

The MCS-based method achieves the highest reliability (94.8% coverage, LOLP = 5.2%) but is more conservative with increased computational burden, yielding a higher mean TRM of 24.01 MW and a lower mean ATC of 191.99 MW.

By contrast, the proposed fully adaptive method achieves a balanced mean TRM of 19.19 MW with a mean ATC of 196.81 MW while exhibiting the widest TRM operating span (47.62 MW) and the highest adaptation ratio (18.8:1). This indicates that simultaneous adaptation of $W(t)$ and $K(t)$ enables prudent margin contraction during stable periods and responsive risk buffering during volatile intervals.

Table 8. Comparative performance of TRM estimation methods.

Metric	Static	Fixed-K	MCS	Proposed Method
Mean TRM (MW)	16.20	18.77	24.01	19.19
TRM Std. (MW)	0.00	4.46	0.76	6.65
TRM Span (MW)	0.00	31.50	5.71	47.62
Mean ATC (MW)	199.80	197.23	191.99	196.81
Coverage (%)	81.80	88.40	94.80	88.0
LOLP (%)	18.20	11.60	5.20	12.0
Adaptation Ratio	1.0:1	8.6:1	1.3:1	18.8:1
Hours Enhanced ATC	0	6.1	0.0	7.50
Computation time (ms)	0.02	2.26	261.75	1.82

4.8. Reliability Preservation and LOLP Validation

Reliability was evaluated using coverage probability and LOLP, defined as the fraction of time steps in which calculated forecast errors exceeded the allocated TRM. As shown in Table 8 and Figure 9, the proposed method increases coverage relative to the

static method (80.0% vs. 81.8%) while remaining computationally efficient. The MCS-based method achieves the highest coverage (94.8%) due to conservative TRM allocation.

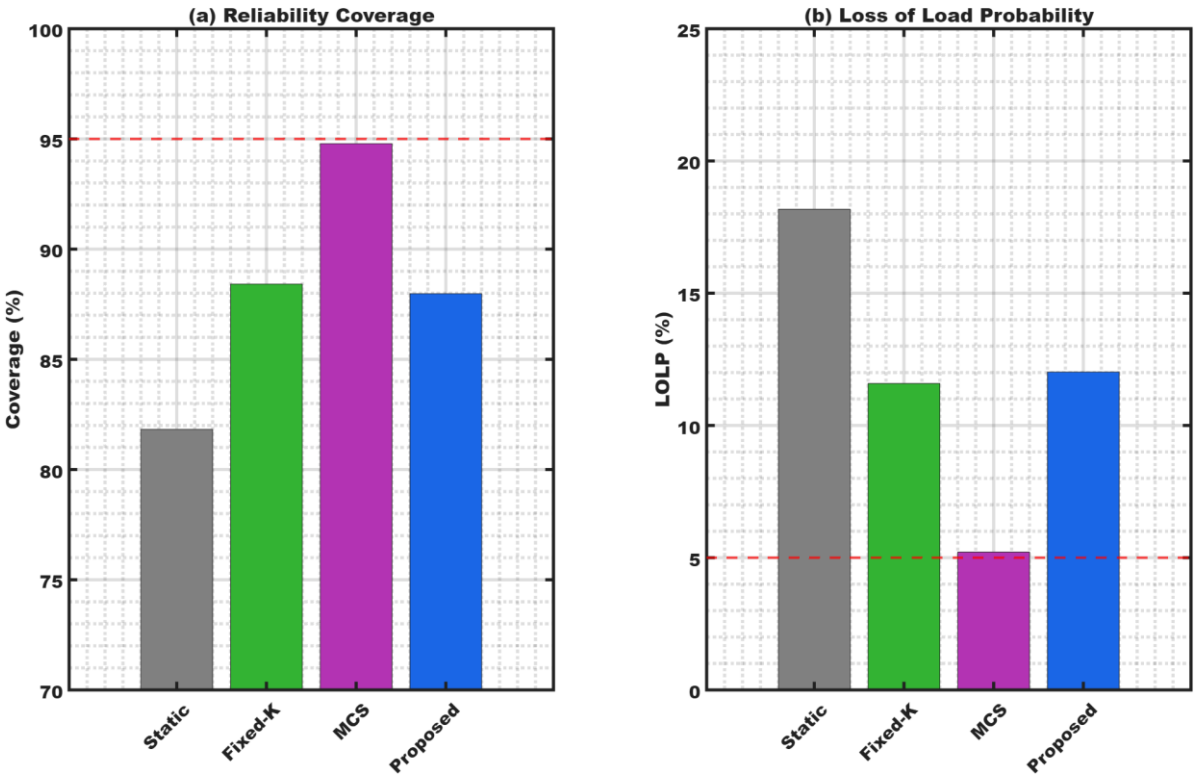

Figure 9. Reliability performance across TRM methods: (**a**) coverage probability and (**b**) Loss of Load Probability (LOLP) for all four methods. The dashed red line indicates the 95% coverage target (equivalently, 5% LOLP).

4.9. Computational Efficiency and Real-Time Feasibility

Average computation times are reported in Table 8. The static method is computationally negligible (0.02 ms). The Fixed-K rolling baseline requires 2.26 ms, and the proposed method requires 1.82 ms, indicating that adaptive confidence adjustment introduces negligible overhead. In contrast, the MCS-based method requires 261.75 ms. Figure 10 presents these timing differences on a logarithmic scale and highlights the substantial computational gap between MCS and rolling-window methods. Overall, the proposed method is approximately 144× faster than MCS, supporting real-time implementation at 1 min update intervals.

4.10. Dynamic TRM Performance of the Proposed Framework

The time-domain behaviors of TRM and ATC are shown in Figures 11 and 12, respectively. The proposed adaptive TRM varies between 2.67 MW and 50.29 MW, corresponding to an adaptation ratio of 18.8:1. This wide operating range demonstrates the framework's ability to dynamically respond to time-varying uncertainty driven by net load forecast errors.

Consistent with this adaptive behavior, the resulting ATC exceeds the static baseline for ~7.5 h, representing 31.5% of the operational day. This indicates improved transmission utilization during low-uncertainty periods, while sufficient reliability margins are preserved during high-volatility intervals.

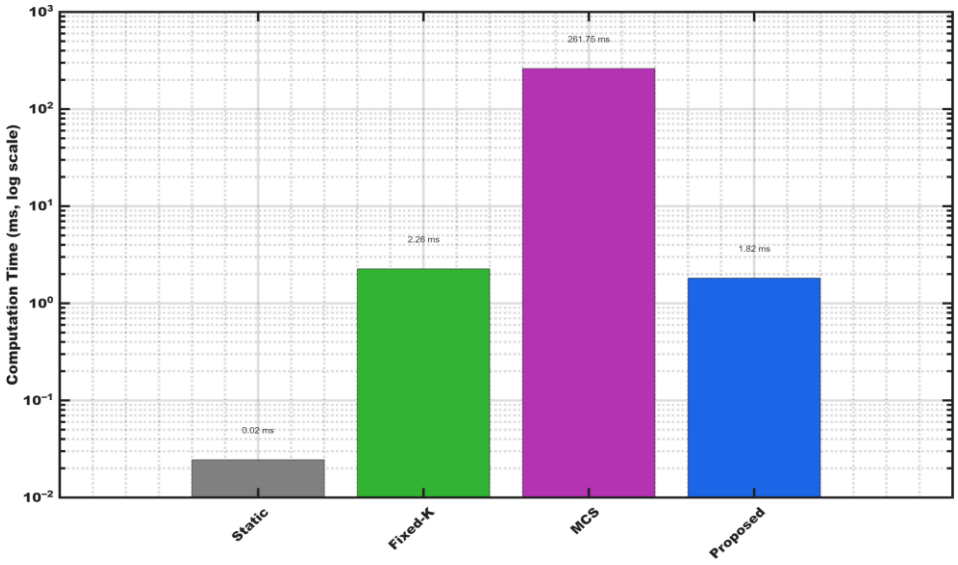

Figure 10. Computation time per 1 min update for all evaluated TRM methods (logarithmic scale).

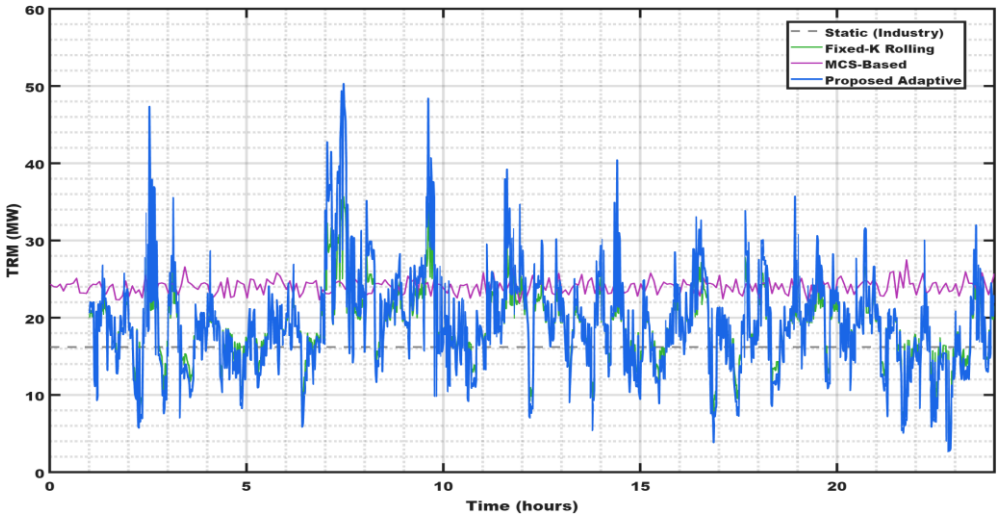

Figure 11. 24 h TRM trajectories for static, fixed-K rolling, MCS-based, and proposed adaptive methods.

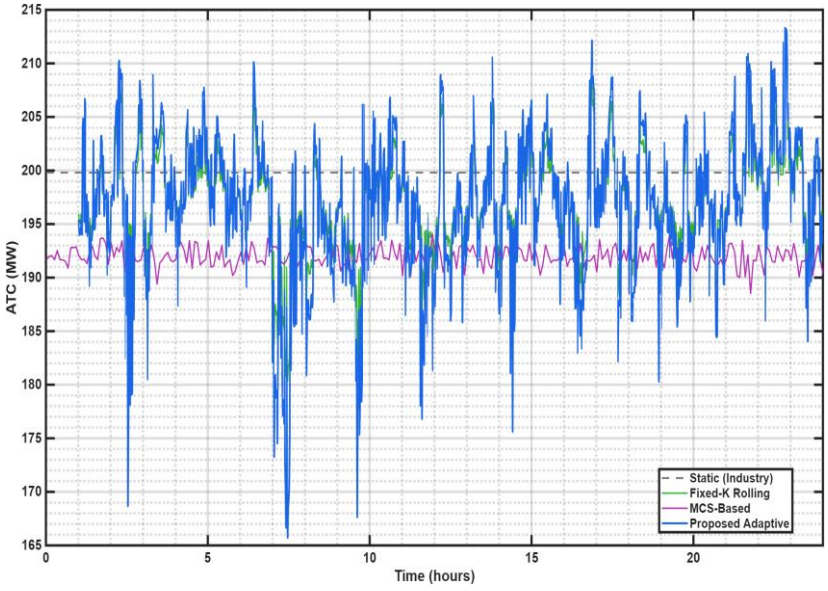

Figure 12. ATC profiles over the 24 h horizon for the four methods (Static, Fixed-K Rolling, MCS-based, and Proposed method).

https://doi.org/10.3390/en19030844

4.11. Effect of Adaptive Confidence Factor $K(t)$

To highlight the contribution of adaptive confidence adjustment, Figure 13 summarizes key performance metrics across methods, while Figure 14 directly compares Fixed-K and the proposed method under the same adaptive window mechanism. The introduction of adaptive $K(t)$ increases the adaptation ratio from 8.6:1 to 18.8:1, while maintaining comparable reliability coverage (88.4% vs. 88.0%), confirming that dual adaptation improves responsiveness without degrading reliability.

4.12. Summary of Key Findings

The proposed fully adaptive TRM estimation framework effectively bridges the gap between static TRM approaches, which are computationally simple but insufficiently responsive, and MCS-based methods, which are reliable but computationally intensive. By jointly adapting the confidence factor $K(t)$ and the rolling window size $W(t)$ based on real-time net-load forecast error statistics, the framework achieves enhanced responsiveness to time-varying uncertainty while preserving system reliability.

For the IEEE 30-bus test system with 42.3% wind penetration, the proposed method yields a mean TRM of 19.19 MW with a dynamic range of 2.67–50.29 MW, corresponding to an adaptation ratio of 18.8:1. Reliability coverage of 88.0% is maintained, comparable to probabilistic benchmarks, while enabling enhanced ATC for 7.5 h (31.5% of the operational day). Compared with the MCS-based TRM, the proposed approach reduces the mean TRM by 20.1% and increases the mean ATC by 2.5%.

Computationally, the adaptive TRM update requires only rolling statistical operations, resulting in a total computation time of 1.82 ms per 24 h cycle for the IEEE 30-bus system. A scalability assessment on the IEEE 118-bus system demonstrates sub-linear computational scaling, with computation time increasing to only 3.61 ms (1.98× increase) despite a 3.93× increase in network size. These results confirm that the proposed framework provides a practical and efficient solution for real-time transmission reliability margin assessment in renewable-rich power systems.

A scalability validation on the IEEE 118-bus system is provided in Appendix A, demonstrating preserved adaptive characteristics (12.4:1 adaptation ratio) with graceful coverage degradation (78.7%) on larger networks.

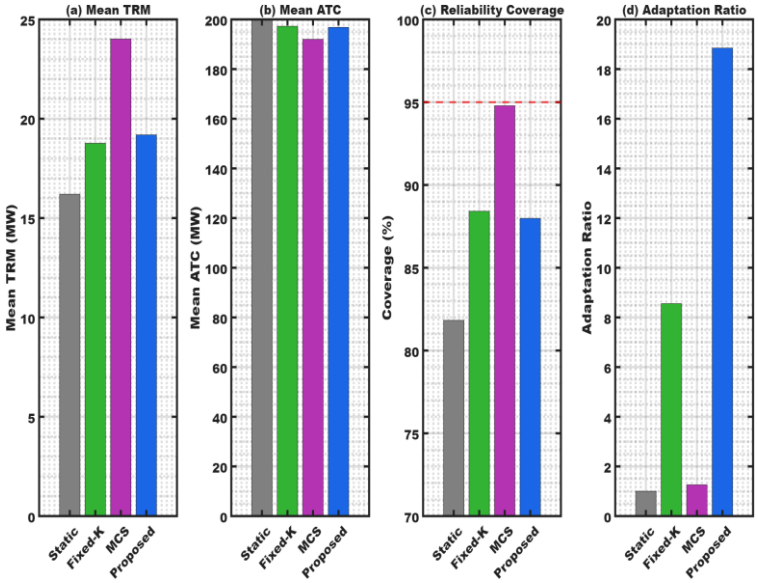

Figure 13. Summary comparison across methods: (**a**) mean TRM, (**b**) mean ATC, (**c**) reliability coverage, and (**d**) adaptation ratio for the static, Fixed-K rolling, MCS-based, and proposed adaptive methods. The dashed red line in (**c**) indicates the target reliability coverage level of 95%.

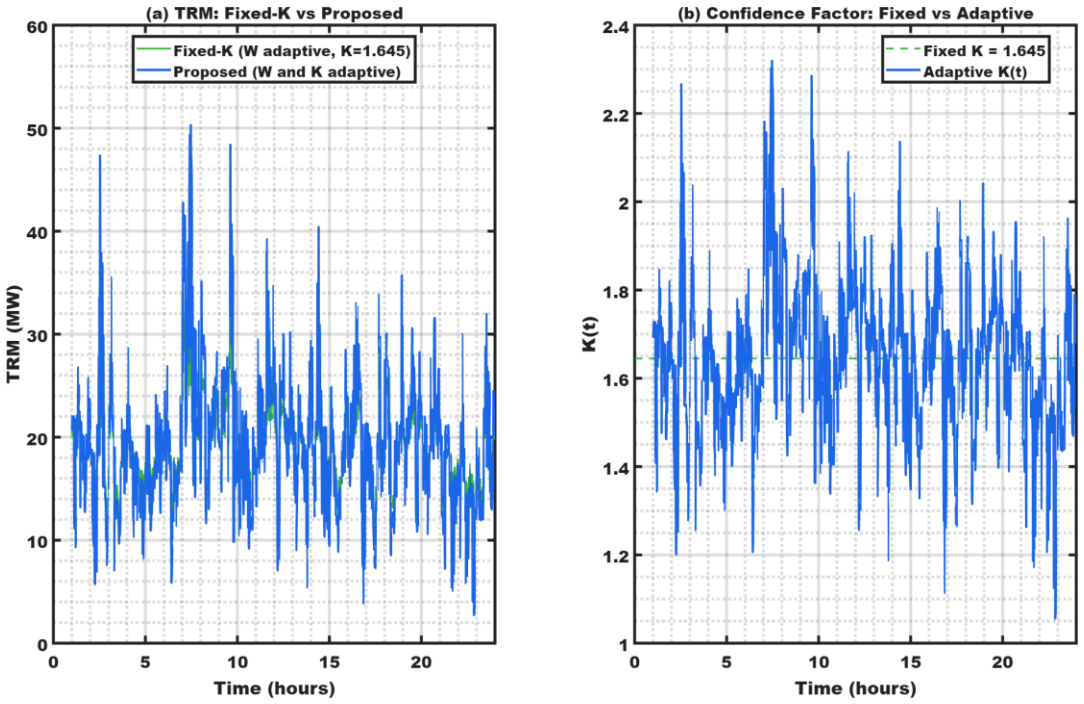

Figure 14. Effect of adaptive confidence adjustment: (**a**) TRM trajectories for Fixed-K (adaptive *W*, $K = 1.645$) versus the proposed method (adaptive *W* and *K*); (**b**) confidence factor comparison between fixed $K = 1.645$ $ and adaptive $K(t)$.

5. Discussion

The comparative results highlight a practical trade-off between reliability and computational feasibility. While MCS achieves the highest coverage (94.8%), its computational cost (261.75 ms) limits it to offline calibration. The proposed method maintains computational efficiency (1.82 ms for 30-bus, 3.61 ms for 118-bus) while enabling margins to respond dynamically to volatility through the adaptive $K(t)$ mechanism.

Adapting $K(t)$ approximately doubles the adaptation ratio relative to Fixed-K (18.8:1 vs. 8.6:1) while preserving comparable coverage (88.0% vs. 88.4%). This indicates that $K(t)$ redistributes TRM over time—contracting margins during stable intervals and expanding them during volatile periods—rather than simply raising average conservatism.

The IEEE 118-bus validation confirms that the framework scales effectively to larger networks. The adaptation ratio is preserved (12.4:1 vs. 18.8:1), TRM-to-TTC proportionality remains consistent (7.0% vs. 8.9%), and computational overhead exhibits sub-linear scaling (1.98× time increase for 3.93× network size increase). The coverage reduction (78.7% vs. 88.0%) reflects increased topological complexity but demonstrates graceful degradation rather than performance collapse.

Several limitations should be acknowledged: the independence assumption between wind and load uncertainties, exclusive reliance on thermal constraints for TTC calculation, and the Gaussian load uncertainty model.

6. Conclusions

This paper presented a fully adaptive TRM estimation framework that combines rolling-window statistical analysis, volatility-responsive window sizing, and an adaptive confidence factor $K(t)$ to track time-varying uncertainty in renewable-rich power systems. The framework was validated on the IEEE 30-bus system with 42.3% wind penetration and assessed for scalability on the IEEE 118-bus system (40.1% wind penetration).

Comparative analysis against static TRM, a Fixed-K rolling baseline, and Monte Carlo Simulation (MCS)-based methods shows that the proposed dual-adaptation

mechanism substantially increases responsiveness while preserving reliability. For the IEEE 30-bus case, the proposed method achieves 88.0% reliability coverage while enabling enhanced ATC for 7.5 h (31.5% of the operational day). Compared with MCS-based TRM, the proposed approach reduces the mean TRM by 20.1% (from 24.01 MW for MCS to 19.19 MW) and increases the mean ATC by 2.5%, with an adaptation ratio of 18.8:1. The IEEE 118-bus validation confirms that the framework scales effectively to larger networks, preserving adaptive characteristics (12.4:1) with graceful coverage degradation (78.7%) and sub-linear computational scaling (1.98× time increase for 3.93× network size increase), supporting real-time minute-by-minute updates.

Future work will investigate the proposed framework on larger networks, incorporate additional sources of uncertainty, such as solar generation and dynamic line ratings, and validate the methodology using utility-grade datasets. In addition, the TTC evaluation stage will be extended to explicitly enforce voltage-security constraints through AC feasibility checks or security-constrained optimal power flow (SCOPF) formulations (e.g., $V^{min}{}_i \le V_i \le V^{max}{}_i$, and correlation-aware multi-source uncertainty modeling will be investigated beyond the temporally persistent net-load error process adopted in this study.

Author Contributions: Conceptualization, U.E.E., T.T.L. and M.A.M.; Methodology, U.E.E., T.T.L. and M.A.M.; Software, U.E.E.; Validation, U.E.E.; Formal analysis, U.E.E.; Investigation, U.E.E.; Data curation, U.E.E.; Writing—original draft, U.E.E.; Writing—review and editing, U.E.E., T.T.L. and M.A.M.; Visualization, T.T.L.; Supervision, T.T.L. and M.A.M. All authors have read and agreed to the published version of the manuscript.

Funding: This research received no external funding.

Data Availability Statement: The original contributions presented in this study are included in the article. Further inquiries can be directed to the corresponding author.

Conflicts of Interest: The authors declare no conflicts of interest.

Appendix A. Scalability Assessment on the IEEE 118-Bus System

To address computational scalability and demonstrate applicability to larger transmission networks, the proposed adaptive TRM framework was additionally evaluated on the IEEE 118-bus test system. This system represents a substantial increase in network complexity relative to the IEEE 30-bus case, comprising 118 buses, 186 branches, and 54 generators.

Appendix A.1. IEEE 118-Bus System Configuration

Wind generation was distributed across 16 buses in the import area (Buses 70–118), resulting in 40.1% wind penetration (1700 MW installed capacity against a total system load of 4242 MW). The transfer corridor was defined between an export area (Buses 1–69) and an import area (Buses 70–118), with the total transfer capability (TTC) computed as 1350 MW based on aggregate inter-area tie-line thermal limits.

To maintain proportional uncertainty consistency with the IEEE 30-bus study, the net-load forecast error standard deviation was calibrated to 5% of TTC (67.5 MW). The baseline confidence factor was set to K_base = 1.96 (95% two-sided confidence) to reflect increased uncertainty propagation paths in a more interconnected network. Adaptive parameters were derived using the same methodology as in the 30-bus case, yielding a reference variability level σ_ref = 38.29 MW, with rolling window bounds retained at 10–60 min and a base window size of W_base = 15 min.

Appendix A.2. Scalability Results

Table A1 summarizes the comparative performance between the IEEE 30-bus and IEEE 118-bus systems. Despite the fourfold increase in network size, the proposed framework preserves its adaptive behavior. For the IEEE 118-bus system, the TRM dynamically varies between 24.05 MW and 297.24 MW, yielding an adaptation ratio of 12.4:1. The resulting mean TRM is 94.17 MW, corresponding to 7.0% of TTC, which is comparable to the proportional margin observed in the 30-bus case.

Table A1. Scalability comparison between IEEE 30-bus and IEEE 118-bus systems.

Metric	IEEE 30-Bus	IEEE 118-Bus	Ratio
Buses	30	118	3.93 ×
Branches	41	186	4.54 ×
TTC (MW)	216.0	1350.0	6.25 ×
Wind Penetration	42.3	40.1	–
Mean TRM (MW)	19.19	94.17	4.91 ×
TRM/TTC (%)	8.9	7.0	–
Adaptation Ratio	18.8:1	12.4:1	–
Coverage (%)	88.0	78.7	–
LOLP (%)	12.0	21.3	–
Computation Time (ms/24 h)	1.82	3.61	1.98 ×

Reliability coverage decreases from 88.0% in the 30-bus system to 78.7% in the 118-bus system, with a corresponding LOLP of 21.3%. This reduction is attributable to increased topological complexity and a larger number of uncertainty propagation paths; however, the framework exhibits graceful degradation rather than performance collapse when applied to a larger network.

Figures A1 and A2 illustrate the time-domain behavior of the proposed method on the IEEE 118-bus system. The TRM trajectory maintains clear responsiveness to time-varying uncertainty, while the adaptive confidence factor K(t) fluctuates around K_{base} = 1.96 and the rolling window size W(t) spans the full operational range of 10–60min, confirming that both adaptive mechanisms remain active at a larger scale.

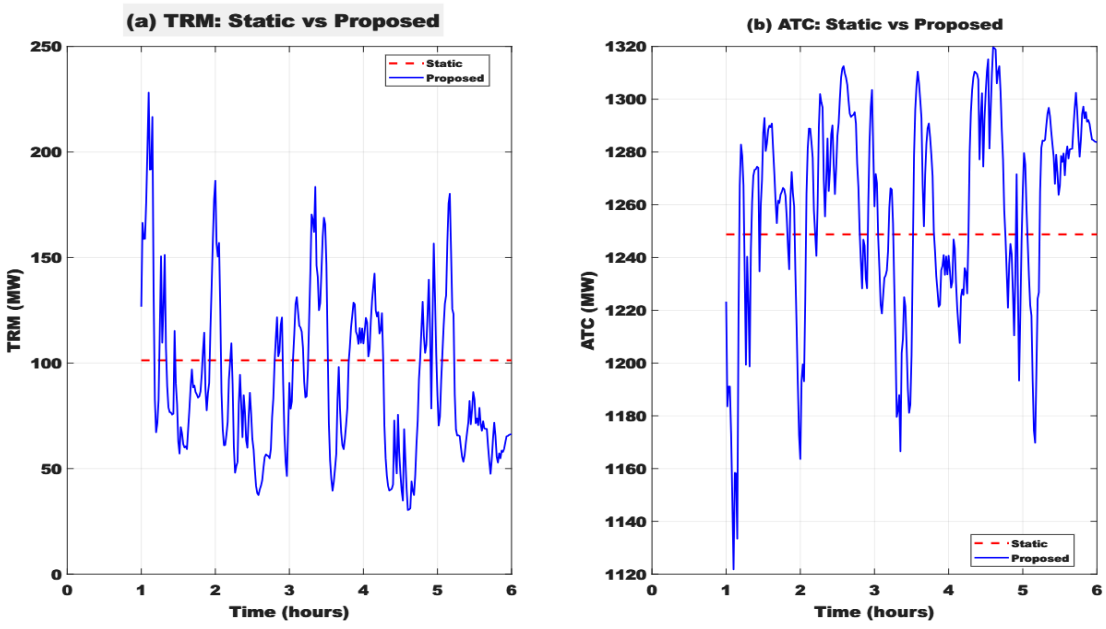

Figure A1. Time-domain trajectories of TRM and ATC over a 24 h horizon for the IEEE 118-bus system using the proposed adaptive framework.

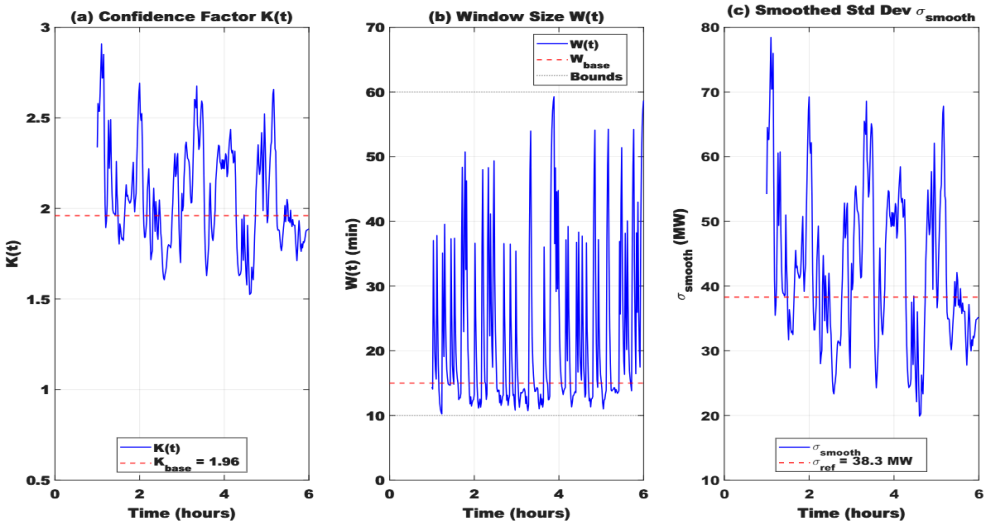

Figure A2. Time evolution of adaptive parameters on the IEEE 118-bus system: (**a**) confidence factor $K(t)$, (**b**) rolling window size $W(t)$, and (**c**) smoothed forecast-error standard deviation σ_{smooth}.

Appendix A.3. Computational Performance

The TRM update step relies exclusively on rolling statistical operations over the forecast-error time series and therefore exhibits computational complexity O(W), where W denotes the window size. As reported in Table A1, the total computation time increases from 1.82 ms (IEEE 30-bus) to 3.61 ms (IEEE 118-bus) per 24 h simulation cycle, representing a sub-linear scaling factor of 1.98× relative to the 3.93× increase in network size.

Figure A3 visualizes this sub-linear computational scaling. The actual computation time (blue line) remains well below the linear reference (red dashed line), indicating that the proposed method does not introduce computational bottlenecks as network size increases. The per-update latency of 0.0026 ms consumes only 0.000004% of the 1 min update budget, confirming real-time feasibility for minute-level updates.

This sub-linear scaling behavior arises because the core TRM update algorithm operates on the forecast error time series rather than on network topology. Extension to transmission networks with 1000+ buses represents an appropriate direction for future validation, potentially leveraging parallel computation for the underlying state estimation and power flow components.

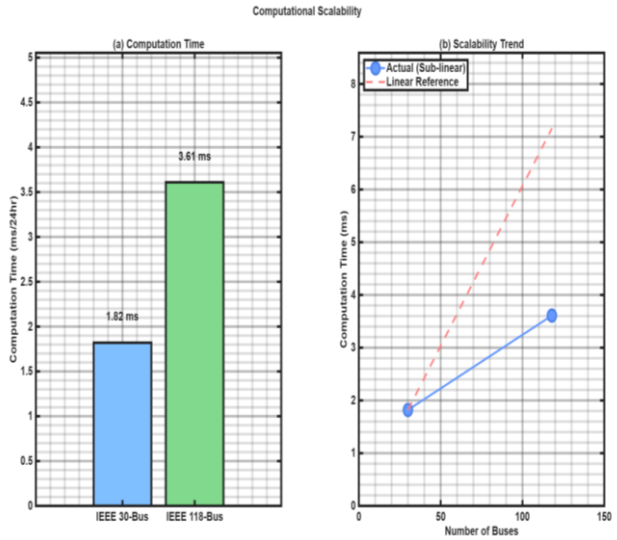

Figure A3. Computational performance of the proposed adaptive TRM framework on the IEEE 118-bus system, demonstrating negligible execution time suitable for minute-level real-time updates.

https://doi.org/10.3390/en19030844

Appendix A.4. Appendix Summary

The IEEE 118-bus evaluation confirms that the proposed adaptive TRM framework scales effectively to larger networks. While reliability coverage shows a moderate reduction due to increased system complexity, the framework preserves its core adaptive characteristics (adaptation ratio 12.4:1) with sub-linear computational scaling (1.98× time increase for 3.93× network size increase), supporting its applicability to practical large-scale transmission systems, as illustrated Figure A4.

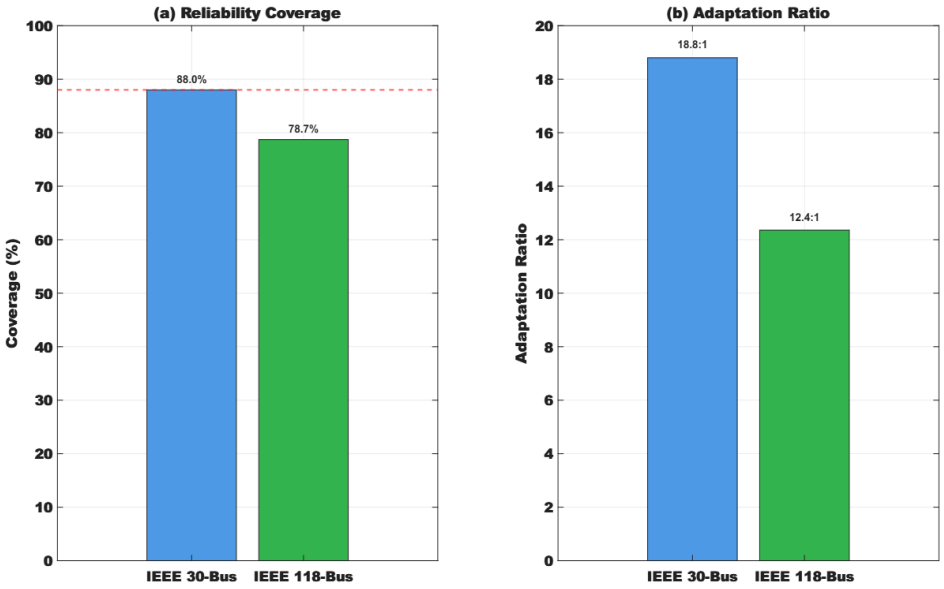

Figure A4. Reliability performance of the proposed adaptive TRM framework, comparing coverage probability and adaptation ratio for the IEEE 30-bus and IEEE 118-bus systems. The dashed red line indicates reliability coverage level of 88%.

References

1. Giebel, G.; Kariniotakis, G. Wind power forecasting—A review of the state of the art. In *Renewable Energy Forecasting*; Woodhead Publishing: Cambridge, UK, 2017; pp. 59–109.
2. Pinson, P.; Kariniotakis, G. Conditional prediction intervals of wind power generation. *IEEE Trans. Power Syst.* **2010**, *25*, 1845–1856.
3. North American Electric Reliability Council. *Available Transfer Capability Definitions and Determination*; Technical Report; North American Electric Reliability Council (NERC): Princeton, NJ, USA, 1996. Available online: https://www.ece.iit.edu/~flueck/ece562/atcfinal.pdf (accessed on 27 October 2025).
4. Kumar, A.; Srivastava, S.; Singh, S. Available transfer capability assessment in a competitive electricity market using a bifurcation approach. *IEE Proc.-Gener. Transm. Distrib.* **2004**, *151*, 133–140.
5. Ou, Y.; Singh, C. Assessment of available transfer capability and margins. *IEEE Trans. Power Syst.* **2002**, *17*, 463–468.
6. Sauer, P.W. Alternatives for calculating transmission reliability margin (TRM) in available transfer capability (ATC). In Proceedings of the Thirty-First Hawaii International Conference on System Sciences, Kohala Coast, HI, USA, 6–9 January 1998; Volume 3, p. 89. https://doi.org/10.1109/HICSS.1998.656069.
7. Ejebe, G.C.; Tong, J.; Waight, J.G.; Frame, J.G.; Wang, X.; Tinney, W.F. Available transfer capability calculations. *IEEE Trans. Power Syst.* **1998**, *13*, 1521–1527. https://doi.org/10.1109/59.736300.
8. McCalley, J.D.; Vittal, V.; Abi-Samra, N. An overview of risk based security assessment. In *1999 IEEE Power Engineering Society Summer Meeting. Conference Proceedings (Cat. No. 99CH36364)*; IEEE: Piscataway, NJ, USA, 1999; Volume 1, pp. 173–178.
9. Edeh, U.E.; Lie, T.T.; Mahmud, M.A. Assessment of Transmission Reliability Margin: Existing Methods and Challenges and Future Prospects. *Energies* **2025**, *18*, 2267.
10. Audomvongseree, K.; Yokoyama, A.; Verma, S.C.; Nakachi, Y. A novel TRM calculation method by probabilistic concept. *IEEJ Trans. Power Energy* **2004**, *124*, 1400–1407.

11. Hakami, A.M.; Hasan, K.N.; Alzubaidi, M.; Datta, M. A review of uncertainty modelling techniques for probabilistic stability analysis of renewable-rich power systems. *Energies* **2022**, *16*, 112.
12. Aien, M.; Hajebrahimi, A.; Fotuhi-Firuzabad, M. A comprehensive review on uncertainty modeling techniques in power system studies. *Renew. Sustain. Energy Rev.* **2016**, *57*, 1077–1089.
13. Billinton, R.; Allan, R.N. *Reliability Evaluation of Power Systems*; Springer Science & Business Media: Berlin/Heidelberg, Germany, 1996.
14. Jordehi, A.R. How to deal with uncertainties in electric power systems? A review. *Renew. Sustain. Energy Rev.* **2018**, *96*, 145–155.
15. Hong, T.; Pinson, P.; Fan, S.; Zareipour, H.; Troccoli, A.; Hyndman, R.J. Probabilistic Energy Forecasting: Global Energy Forecasting Competition 2014 and Beyond. *Int. J. Forecast.* **2016**, *32*, 896–913.
16. Li, W. *Reliability Assessment of Electric Power Systems Using Monte Carlo Methods*; Springer Science & Business Media: Berlin/Heidelberg, Germany, 2013.
17. McKay, M.D.; Beckman, R.J.; Conover, W.J. A Comparison of Three Methods for Selecting Values of Input Variables in the Analysis of Output from a Computer Code. *Technometrics* **1979**, *21*, 239–245. https://doi.org/10.2307/1268522.
18. Helton, J.C.; Davis, F.J. Latin hypercube sampling and the propagation of uncertainty in analyses of complex systems. *Reliab. Eng. Syst. Saf.* **2003**, *81*, 23–69.
19. Othman, M.; Musirin, I. A novel approach to determine transmission reliability margin using parametric bootstrap technique. *Int. J. Electr. Power Energy Syst.* **2011**, *33*, 1666–1674.
20. Xu, Y.; Valinejad, J.; Korkali, M.; Mili, L.; Wang, Y.; Chen, X.; Zheng, Z. An adaptive-importance-sampling-enhanced Bayesian approach for topology estimation in an unbalanced power distribution system. *IEEE Trans. Power Syst.* **2021**, *37*, 2220–2232.
21. Holttinen, H.; Kiviluoma, J.; Helistö, N.; Levy, T.; Menemenlis, N.; Liu, J.; Cutululis, N.; Koivisto, M.; Das, K.; Orths, A.; et al. *Design and Operation of Energy Systems with Large Amounts of Variable Generation: Final Summary Report, IEA Wind TCP Task 25*; VTT Technical Research Centre of Finland: Espoo, Finland, 2021.
22. Wang, Z.; Bu, S.; Wen, J.; Huang, C. A comprehensive review on uncertainty modeling methods in modern power systems. *Int. J. Electr. Power Energy Syst.* **2025**, *166*, 110534.
23. Edeh, U.E.; Lie, T.; Mahmud, M.A. Dynamic Transmission Reliability Margin Assessment Using Rolling Window Statistical Analysis for Enhanced Available Transfer Capability. In *2025 IEEE Region 10 Symposium (TENSYMP)*; IEEE: Piscataway, NJ, USA, 2025; pp. 1–6.
24. Bifet, A.; Gavalda, R. Learning from time-changing data with adaptive windowing. In *Proceedings of the 2007 SIAM International Conference on Data Mining*; SIAM: Philadelphia, PA, USA, 2007; pp. 443–448.
25. Wen, K.; Wu, W.; Wu, X. Electricity demand forecasting and risk management using Gaussian process model with error propagation. *J. Forecast.* **2023**, *42*, 957–969. https://doi.org/10.1002/for.2925.
26. Celik, A.N. A statistical analysis of wind power density based on the Weibull and Rayleigh models at the southern region of Turkey. *Renew. Energy* **2004**, *29*, 593–604. https://doi.org/10.1016/j.renene.2003.07.002.
27. Shu, Z.; Jirutitijaroen, P. Latin hypercube sampling techniques for power systems reliability analysis with renewable energy sources. *IEEE Trans. Power Syst.* **2011**, *26*, 2066–2073.
28. Inoue, A.; Jin, L.; Rossi, B. Rolling window selection for out-of-sample forecasting with time-varying parameters. *J. Econom.* **2017**, *196*, 55–67. https://doi.org/10.1016/j.jeconom.2016.03.006.